

FIBER OPTICS IN BONDED REPAIRS

Angela Trego, Ph.D., P.E.
Russell Keller
The Boeing Company
PO Box 3999 MS 84-09
Seattle, WA 98124-2499

ABSTRACT

The structural aerospace community has historically struggled in relying on bonded structural repairs for restoration of damaged aircraft components, even though the bonded repair technique shows high potential in extending the structure's life. The primary reason is that the capability and durability of the as-installed repair cannot be quantified. Two things can be said about the repair – that it was installed according to the written procedures and that a non-destructive inspection revealed no unacceptable defects. These two facts, unfortunately, do not guarantee the repair will fulfill its intended purpose. Consequently, severe limits are imposed on the size of bonded repairs, mechanically fastened repair techniques are used instead, or the component is replaced.

A verifiable way of measuring a bonded repair's performance is needed. This paper discusses the feasibility of installing fiber optic strain sensors within a bonded patch repair to measure the ability of the patch to transfer load through the adhesive bondline and patch and verify the repair's performance. Data was successfully obtained from sensors embedded in both coupon and patch specimens during bending and impact loading conditions. An assessment of the results is discussed as well as issues remaining for installing and obtaining the data during operational use.

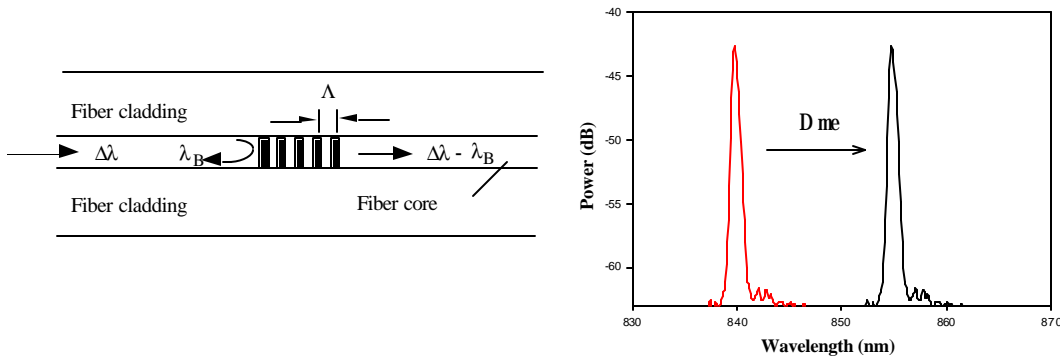
KEY WORDS: Bonded Repair, Fiber Optic Sensors, Non-Destructive Inspection (NDI)

1. INTRODUCTION

To address the need for in-situ sensors to nondestructively monitor the health of a bonded structural repair patch and hard to inspect metallic and composite structural regions, optical fiber strain and chemical sensors are being developed and applied to detect and/or monitor deterioration of these areas. This includes the ability to detect and monitor water penetration and corrosive activity (as in the case of a hard-to-inspect area), as well as delaminations, disbonds, and load bearing capability. The primary objective is to detect and monitor any damage growth while still below the critical damage limits of the structure.

The sensing system is comprised of optical fiber Bragg gratings-based strain sensors. These sensors may be multiplexed with other Bragg grating-based sensors as well as long period grating-based chemical sensors [1] and embedded within the bonded joint, composite structure or the repair patch for structural health monitoring. Both the Bragg and the long period grating sensor have similar signal-conditioning techniques that can be incorporated into a single monitoring system for simultaneous interrogation of multiple sensors. The development of low profile, distributed, embeddable, real-time, optical fiber sensors capable of detecting the onset of bonded joint or patch failure on repaired regions of the aircraft would eliminate a significant portion of the related maintenance costs as well as improve confidence levels in the technology, so that widespread implementation of the technology may proceed.

1.1 Sensor Design Photo induced Bragg gratings were first demonstrated by K.O. Hill et al. in 1979 [2] using light from an argon-ion laser. Currently, the optical fiber Bragg grating is fabricated by exposing UV light through a phase mask onto the optical fiber. This fabrication process offers the capability of maintaining the pristine ultimate strength of the optical fiber by recoating Bragg grating sensors with a protective polymer after the writing process. Inherent advantages that optical fiber Bragg grating strain sensors have over the foil strain gauge include size and flexible geometry, resistance to EMI, sparks, and most chemicals, and allowance for inexpensive distributed sensing capabilities. As opposed to the foil strain gauge, the Bragg grating strain sensor operates on self-referencing absolute measurements. This allows the user to unplug and plug into the sensor at time-based intervals without having to recalibrate. The resulting sensor element is illustrated below, in figure 1a, along with the optical spectrum shift with strain in figure 1b.



a) Refractive index variation within the core b) Spectral shift with induced strain
Figure 1. Schematic of the Bragg Grating Sensor

As shown in figure 1a, the photo-induced planes of constant index of refraction will be oriented perpendicular to the axis of the fiber. In this configuration, part of the light incident on the grating gets back reflected while most of the light will be transmitted. The reflected wavelength, λ_B , will interfere constructively after reflecting off each of the layers, satisfying the Bragg equation relationship:

$$\lambda_B = 2n\Lambda, \quad (1)$$

where n is the index of refraction, and Λ is the grating spacing. If strain is applied to the Bragg grating, the resonant reflected wavelength λ_B will shift by an amount given by $\Delta\lambda_B$, where:

$$\Delta\lambda_B/\lambda_B = (1 - P_E)\epsilon, \quad (2)$$

where P_E is the photo elastic constant for the silica fiber core. Hence by tracking $\Delta\lambda_B$, residual strain can be accurately monitored. Figure 1b illustrates strain measurements using the spectral shift from a Bragg grating.

Blue Road Research, in cooperation with The Boeing Company, has performed studies on adhesive bondline failures. It has been found that the multi-axis fiber grating strain sensors provide information about transverse strain, axial strain, and transverse strain gradients that can provide important information throughout the adhesive joint. By changing the orientation of the sensor, shear strain and its effects can be clearly measured. In one study [3], aluminum double lap adhesive joints were instrumented with multi-axis sensors and subjected to tension and fatigue tests. Each specimen contained one sensor located either near the bond (retrofit), embedded at the edge of the bond, or embedded towards the inner bond area. Of these three sensor locations, the retrofit was the most promising due to the fact that it allows for existing joints to be instrumented for health monitoring. The main mechanical action in an adhesive joint is shear, and the multi-axis sensor can be used to measure shear strain by orienting the transverse strain sensing axes of the sensor in the shear direction. Thus, as the joint is loaded, the shear in the joint will apply a measurable transverse load on the embedded sensor. The joints with sensors embedded into the adhesive showed minimal strength degradation. The embedded sensors also showed a capability to withstand large strain fluctuations in the joint and in many cases surviving beyond joint failure.

Luna Innovations tested fiber optic sensors in lap shear coupons to demonstrate the feasibility of using Bragg gratings inside adhesive joints [4]. Type I single lap shear specimens, containing 80 and 125-micron diameter Bragg grating based strain sensors embedded within the adhesive bondline, were fabricated in accordance with Boeing Specification BSS 7072. The purpose was to demonstrate the measurement of strain and load bearing capability of the adhesive bondlines before and after environmental exposure in 98% RH/60 °C for 90 days. For real-time data acquisition a prototype signal conditioning system with a laptop computer interface was used to interrogate the Bragg grating response by tracking the spectral shift of the reflected wavelength. The demonstrated Luna Prototype system can track a Bragg grating wavelength shift with a resolution of 1 picometer. This gives an estimated sensitivity of the overall system to measure strain changes on the order of 1.5 $\mu\epsilon$. The test specimen results represented behavior in adhesive joints, composite patch repairs, and composite structural areas.

2. Evaluation Plan and Results

A two-phase evaluation plan was conducted for this study. The first phase verified that the fiber optic sensors could be installed in a coupon's adhesive bondline without breaking and then used to measure strains upon loading. The sensors were installed in a realistic field repair approach rather than a laboratory environment. The second phase shows the feasibility of installing and using the sensors in two different repair applications.

2.1 Phase 1 Coupon Installation Test coupons containing fiber optic sensors were fabricated and tested to verify the ability to install and detect changes in the sensor output during loading. Axial and bi-axial fiber optic Bragg-grated strain sensors were installed in the bondline joint of

two 1.6 mm (0.063”) thick aluminum (7075-T6 and 2024-T3 alloys) panels, assembled such that a “stabilized” wide area single lap joint of the two panels was created. Figure 2 illustrates the specimen configuration. The lap joint was 10 cm (4 inches) wide by 5 cm (2 inches) long for two primary reasons: 1) the extended width provided a large bonded area around the sensor that would correlate to the area in a bonded doubler situation, and 2) to accommodate an easier installation of the fiber optic sensor in the joint. Unlike previous efforts at installing fiber optic sensors where the fibers were installed across the joint, these sensors were placed in parallel to the load direction. The sensors were installed in the longitudinal center of the joint (for “C-x” labeled specimens) and at the longitudinal edge of the joint (for “E-x” labeled specimens). Figure 3 shows the sensor installation locations and figure 4 shows pictures from the specimen fabrication.

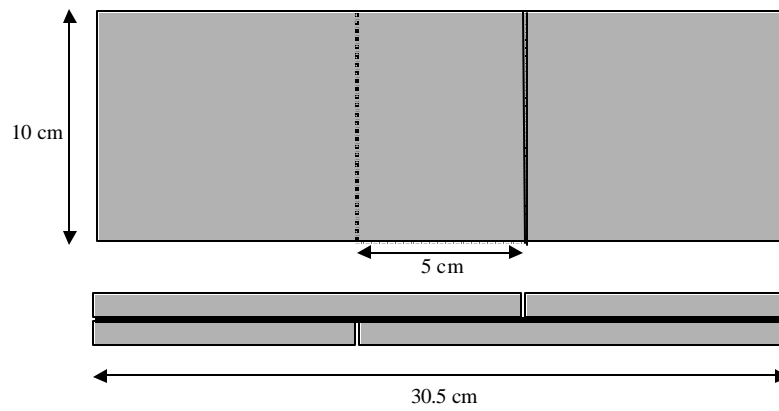


Figure 2. Single Lap Shear Specimen Configuration

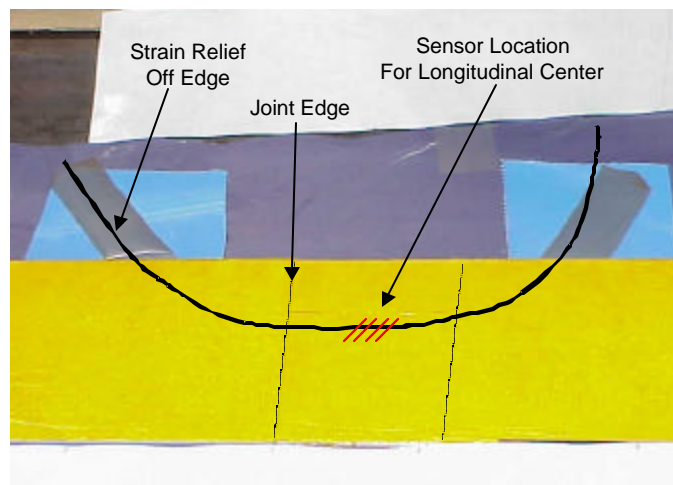


Figure 3. Fiber Optic Strain Sensor Orientation and Locations

Because these specimens were to be tested in tension using pressure grips to hold the ends, the optic fiber was brought into the joint from the side of the specimen beyond the point at which the grips would squeeze the specimen. Nylon tape extending out from the sides of the bottom panel provided strain relief for the optic fibers. The optic fibers were arced to allow the fiber on and back off the panel. The adhesive used to bond the specimens together was Cytec’s 0.25 mm thick FM-73M OST film adhesive.

The specimens were placed in a vacuum bag and cured under full vacuum using a heat blanket and hot bond controller. The cure cycle for bonding was at 121°C for 90 minutes under full vacuum. Because previous data showed very little response to moisture conditioning, these initial specimens were not conditioned. The primary goal was to have the sensors survive the vacuum bag and handling process and then collect data from them under load as the specimens were being tested. Three of the specimens had the sensor in the joint center with two of these being a single axis sensor (C1 and C1A). The third specimen had a bi-axial sensor (C2). The fourth specimen fabricated, E2, had a bi-axial sensor installed near the edge of the joint.

The specimens were tested in the load frame shown in figure 4. Load and head displacement data was collected throughout the test. Load control vs. a head displacement rate was used in order to take sensor readings at specified applied load levels periodically. An optical spectrum analyzer (OSA) was used to record the sensor data. After the specimen was aligned in the grips, an initial reading of the sensor data was obtained. The grip pressure was then applied and another sensor reading was taken to ensure there was no adverse affect or shift in the sensor reading due to the grip pressure. Additional sensor readings were taken at specified load levels. The loading was temporarily halted (approximately one minute) for each reading.

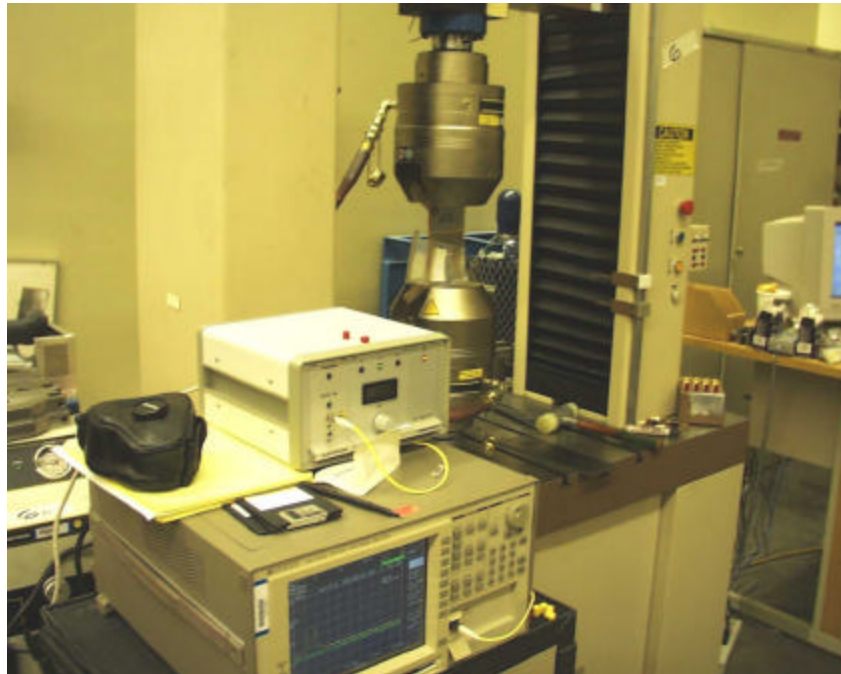
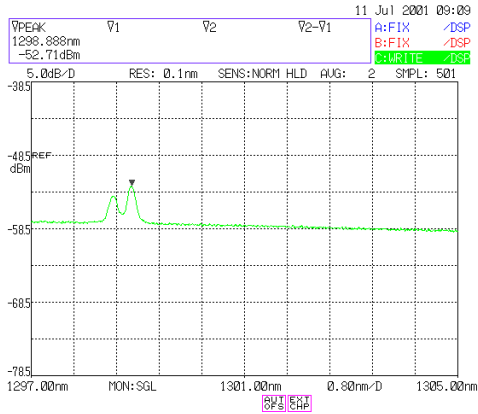
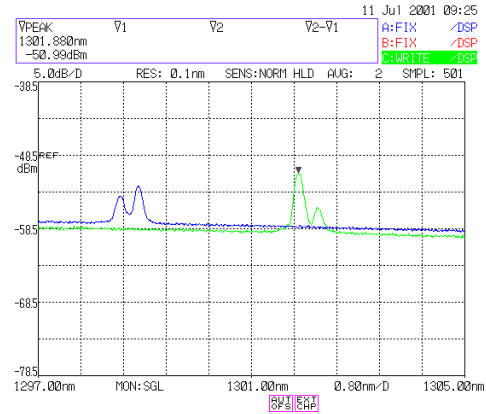


Figure 4. Test Set-up with OSA for Sensor Data Recording

Data could be obtained from each specimen. Changes in the sensor data could be seen real-time by displaying the initial wavelength output as a phantom curve on the graph. Then, as new readings were taken and recorded, the shift in the wavelength peaks could be observed on the OSA screen. Figure 5 shows a typical screen display of the initial response and the shift at the recorded load.



Initial Data Before Load Applied



Wavelength Shift Under Load

Figure 5. C2 Coupon Sensor Data Recorded Before and During Loading

The wavelength output from the sensors indicates relative strain measurements. As can be seen, the data shows a strong shift to the right as well as a change in peak magnitudes. The peak magnitude changes only mean that the polarization is being affected, but does not effect a wavelength-based measurement. The correlation between axial strain and wavelength change is the Bragg equation, equation (2), which relates the Bragg wavelength and wavelength shift to a constant times the strain. The photo elastic constant for these fibers is not available at this time, but will need to be obtained in order to make use of the recorded data for structural evaluation.

Table 1 provides a summary of the coupons tested, observations and results. It must be acknowledged that the specimen configuration was not optimum for lap shear testing, as the aluminum plates were not thick enough for the bonded area tested. Consequently, each specimen experienced substantial bending above and below the joint. This, in turn, introduced out-of-plane loading conditions and the coupons broke at the edge of the lap joint. Thus, no correlation can be made of the wavelength changes to shear strains. The bending also imposed high strains on the optic fibers themselves and broke all but one (C2) of them just prior to specimen failure.

Table 1. Summary of Lap Shear Test Results and Sensor Data

Specimen	Sensor Type	Sensor Location	Max Load (Kilonewtons)	Test Observations
C1	Axial	Center	80.26 (No Failure)	Small cracking sound just before peak lost at 77.7 kN. Test stopped before failure.
C1A	Axial	Center	79.40	Small cracking sound just before peak lost at 74.4 kN. Coupon broke at the butt joint.
C2	Bi-Axial	Center	78.95	Good axial readings but poor transverse readings. Small cracking sound just before coupon broke. Sensor survived.
E2	Bi-Axial	Edge	79.85	Good axial readings but poor transverse readings. Small cracking sound just before losing peak at 76.1 kN. There may be a slight inclination of part failure as the two peaks begin to merge, but nothing conclusive from the one test specimen.

Figures 6 and 7 contain data outputs from the sensors installed in coupons C1 and C2 respectively. A representative plot of the wavelength shift during loading is shown, wherein the original wavelength output is overlaid onto an output recorded during loading. The data recorded from the axial sensor (figure 6) shows the wavelength shift in the peaks. Figure 7 of the bi-axial sensor records two wavelength peaks. As can be seen in this sensor, the separation of the two peaks did not change much for either the C2 or E2 sensor. It is interesting to note that the maximum amplitude of the two peaks for both biaxial sensors switched from the right peak to the left peak as the coupon was loaded, however, this phenomenon is not significant to strain correlation.

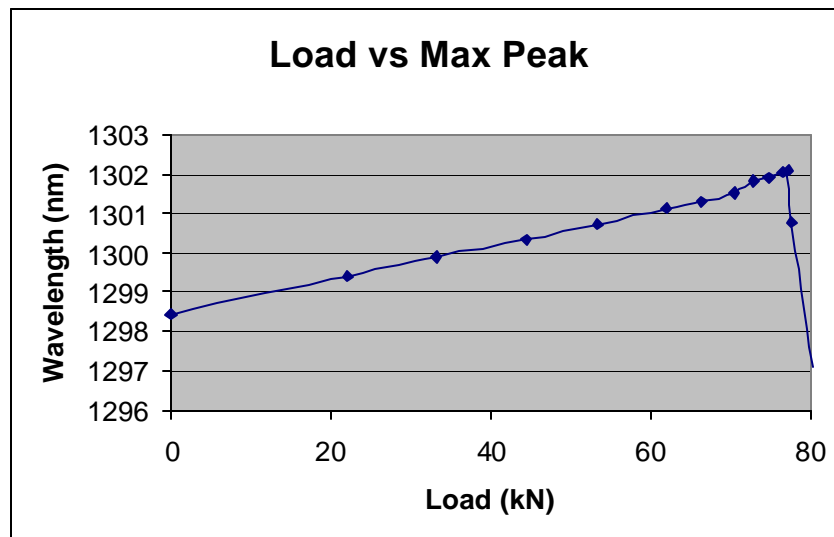
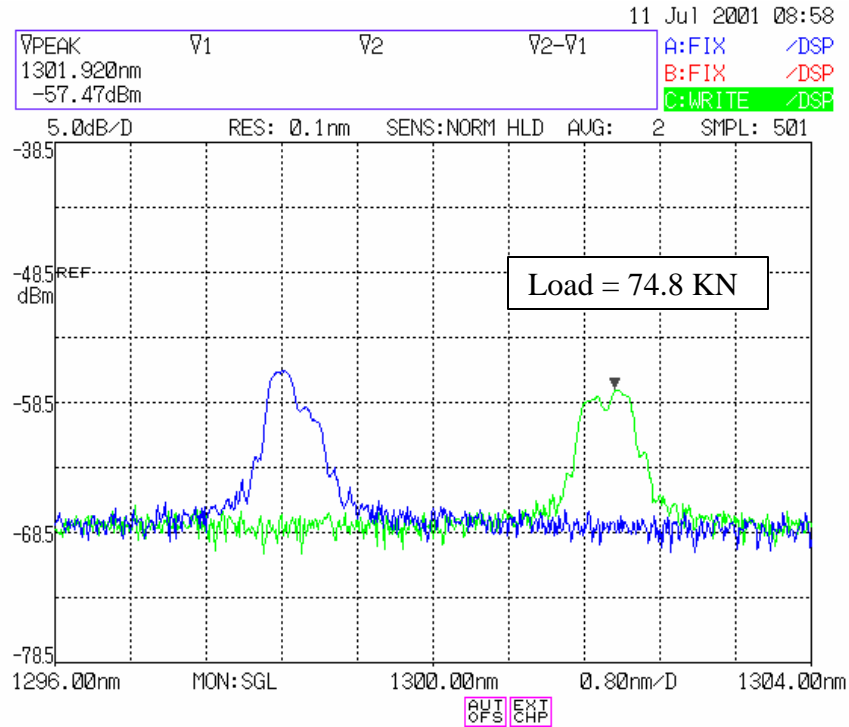


Figure 6. C1 Wavelength Output and Load vs Max Peak

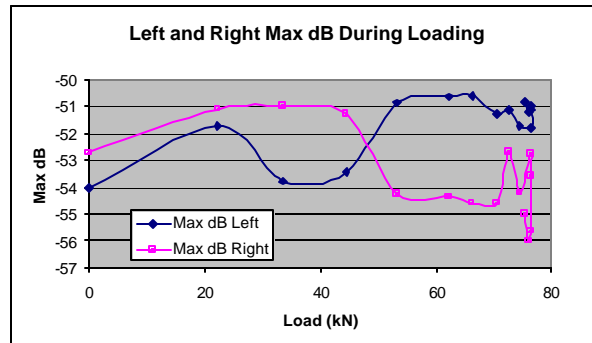
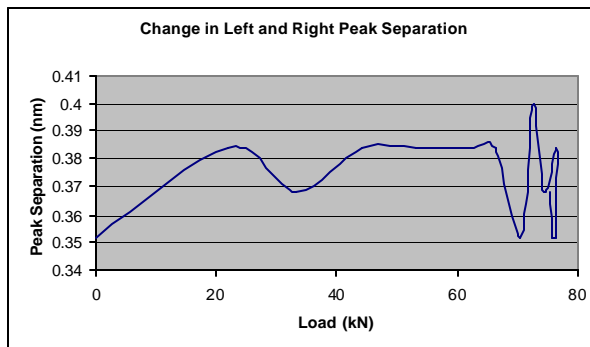
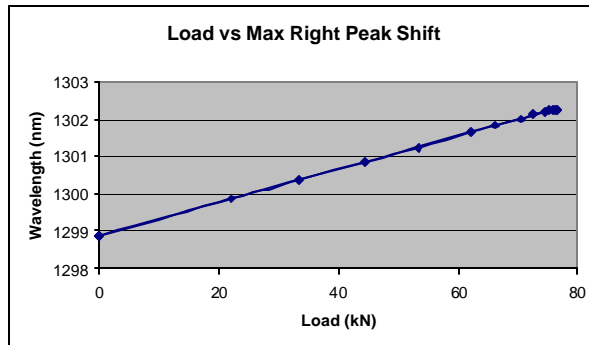
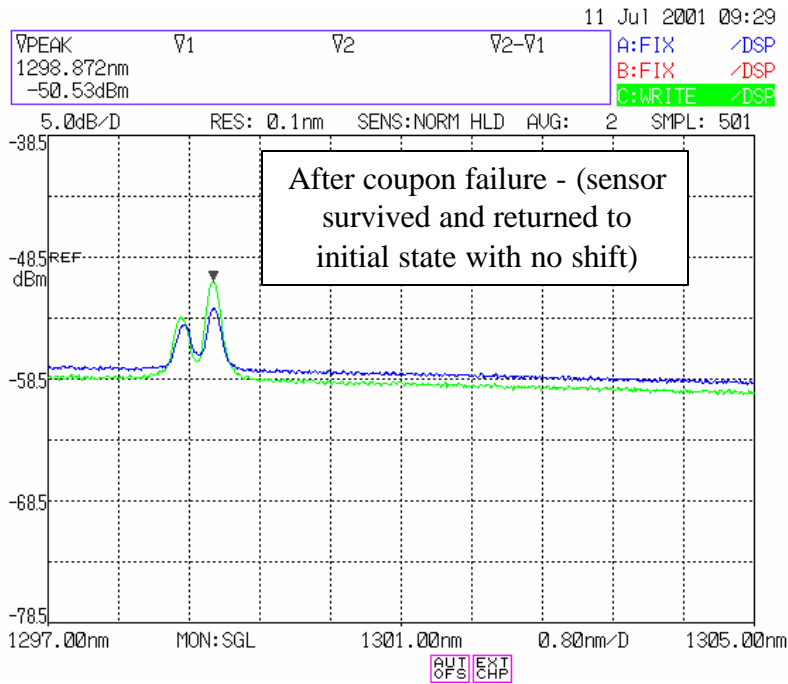


Figure 7. C2 Wavelength Output and Peak Data

From this testing several conclusions can be made. The optic fiber installation method used was successful in terms of sensor survival after fabrication and during test. The tests were also successful based on being able to obtain sensor readings throughout the tests, even up to and beyond (in one case) failure. The sensor output indicates a wavelength shift as the specimens

were loaded. The change in wavelength along the axial direction for each of the fibers was consistent with the change in applied load overall as seen in Table 2.

Table 2. Comparison of Sensor Wavelength Change and Applied Load

Specimen	Wavelength Change	Load Change
C1	3.65 nm	74.4 KN
C1A	2.91 nm	74.4 KN
C2	3.35 nm	76.3 KN
E2	3.80 nm	79.8 KN

In the case of the specimens with bi-axial sensors, both wavelength peaks were recorded. However, a negligible level of change in peak separation throughout the testing occurred, which indicates that the sensor is not adequately measuring a change in shear strain. In addition, just prior to failure, all but one of the sensors failed. This could have been good in that it may be indicating specimen failure in the bonded lap joint, however, this was not the case as the specimens did not fail in this area but failed at the butt joint of one of the adherends. These results initially suggests that placement of the bi-axial sensors in this configuration (running along the load path, perpendicular to the bondline in a 45 degree orientation) does not produce sufficient output signal to indicate changes in the shear strain in the bondline. Unfortunately, these results are not conclusive, as the coupons did not fail in the bondline due to the excessive bending. A properly designed specimen, where the failure occurs in the bondline (adhesively or cohesively), may have a better wavelength signal output indicating shear strain changes. It should also be noted that if the optic fibers were placed across the bond (perpendicular to the load as done previously by both Blue Road Research and Luna Innovations) the fiber would not have broken, but it also is not aligned with the primary loading direction and would not sense the critical strains that lead to failure.

2.2 Phase 2 Component Installations Using the experience gained on the installation technique(s) evaluated in Phase 1, optic fiber Bragg-grating sensors were installed on two different structural components. The primary objective was to verify that the installation techniques used are feasible on actual structural applications. The two different types of components selected were an aluminum fuselage panel and an upper engine bay honeycomb panel fabricated with graphite/bismaleimide composite material.

The fuselage panel was mounted on a stand in the vertical position. This enabled the evaluation of installing the sensors in a vertical position. A 23 cm by 23 cm area of the panel, between stiffeners, was chosen for installation of an externally bonded-on boron/epoxy doubler. The aluminum surface was anodized and primed using the Phosphoric Acid Anodizing Containment System (PACS) and BR-127 epoxy primer. The patch was a five-ply unidirectional patch that was 15 cm wide by 20 cm long and was bonded on using FM-73M OST epoxy film adhesive and a heat blanket, vacuum bagged process. Two axial Bragg-grated fiber optic sensors were installed with the patch. One sensor was placed in the bondline and the other sensor was placed under the top layer of the patch. Figures 8 and 9 show the patch installation and a schematic of the sensor placement, respectively.

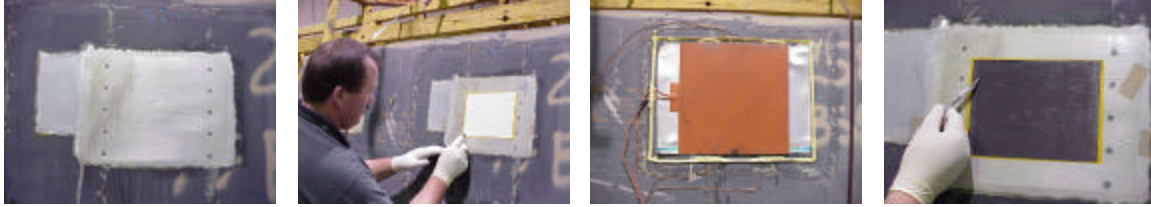


Figure 8. Boron/Epoxy Patch and Sensor Installation on Fuselage Panel

Immediately after fabrication, the sensors were checked for functionality. Both appeared to work, however, upon testing (which occurred several weeks later), the top sensor was inoperative. The cause was not known. Fortunately, the bottom sensor still worked properly. Initially, the patch was impacted with a hammer to see if the optic fiber sensor could detect the impact force and if the sensor would survive. The OSA instrumentation could not respond quickly enough to pick up the impulse loading, however, the sensor did survive. A heat gun was then applied to the patch near the sensor. Two thermocouples were also placed in the area to record the local temperature, one in the middle of the patch and the other on the metal near the sensor location. Only the metal thermocouple near the sensor location was recorded. Heat was then applied to the patch. Readings from the sensor was recorded as the temperature was increased to almost 149°C and as the part cooled down. The recording of the sensor output and temperature were done manually.

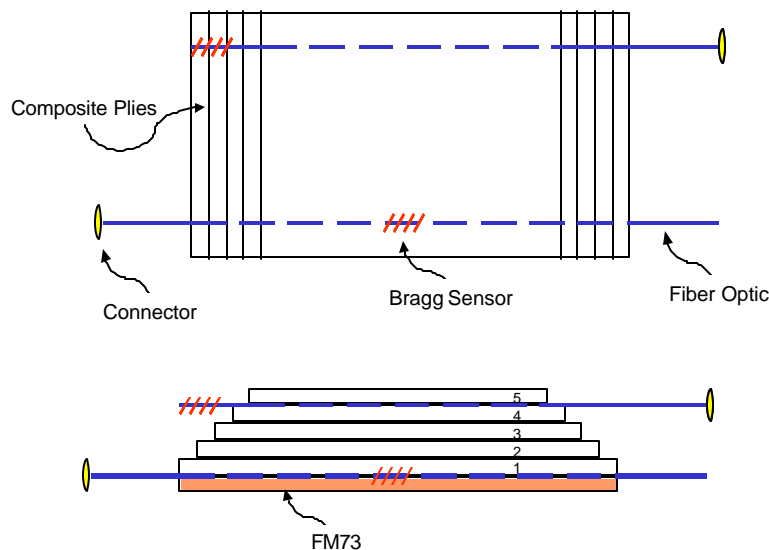


Figure 9. Fuselage Panel Patch and Sensor Installation Schematic

A plot of the maximum wavelength peak and temperature is shown in figure 10. The first measurement at 33°C was not at a steady state temperature. Also, the part heated up rapidly while the cooling down process was much slower. For example, it was approximately 5 seconds between the first (33°C) and second reading (93°C) and it was approximately two minutes between the fifth (83°C) and sixth (72°C) readings. So, between the time of recording data and calling out the temperature, the peak could have shifted on the heating side. This may also be why there appears to be a hysteresis of sorts in the temperature plot.

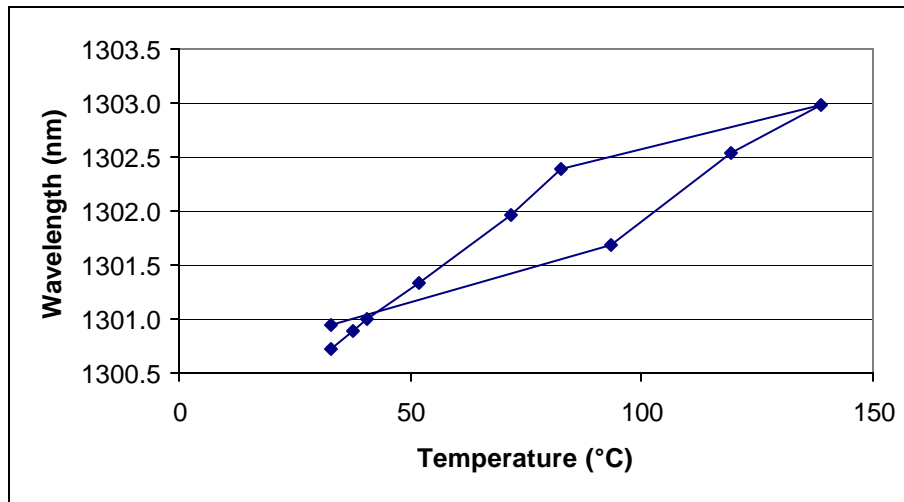
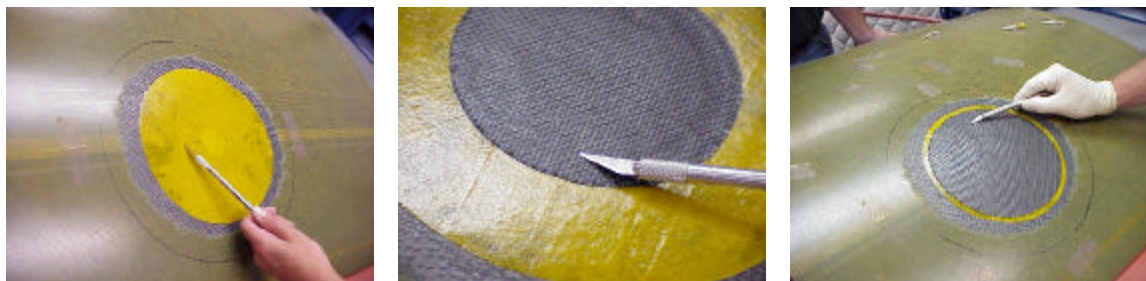


Figure 10. Fuselage Panel - Wavelength Peaks at Different Temperatures

The composite panel used was a composite honeycomb panel made from graphite/ bismaleimide (BMI) prepreg material and has a compound curvature. A highly curved area of the honeycomb panel was chosen for the repair area. The skin in this area was determined to be approximately 18 plies of fabric. A scarf with a 20:1 scarf ratio was sanded in the skin that resulted in a 20 cm diameter circle. The intent of this installation trial was twofold; to verify the installation methods and to record the sensor readings during a loading event. Because this repair was not to be structurally tested for strength, a 121°C cure graphite/epoxy fabric patch was applied to minimize the overall cure time and eliminate any high temperature (190-230°C in this case for BMI) heat-up problems that might have been encountered. These high temperatures may have also damaged the optic fiber sensors and connectors. Again, FM-73M OST film adhesive was used to bond on the patch.

Three Bragg-grated axial fiber optic sensors were installed in this scarfed patch, one in the bondline and two within the patch. Figures 11 and 12 show the patch and sensor installation and the sensor installation schematic, respectively. Note that the sensors in this patch are installed in different directions to evaluate the ability to distinguish wavelength output differences due to different levels of strain.



Sensor in Bondline

Sensor Between Plies

Sensor Near Top

Figure 11. Composite Panel Scarfed Patch and Sensor Installation

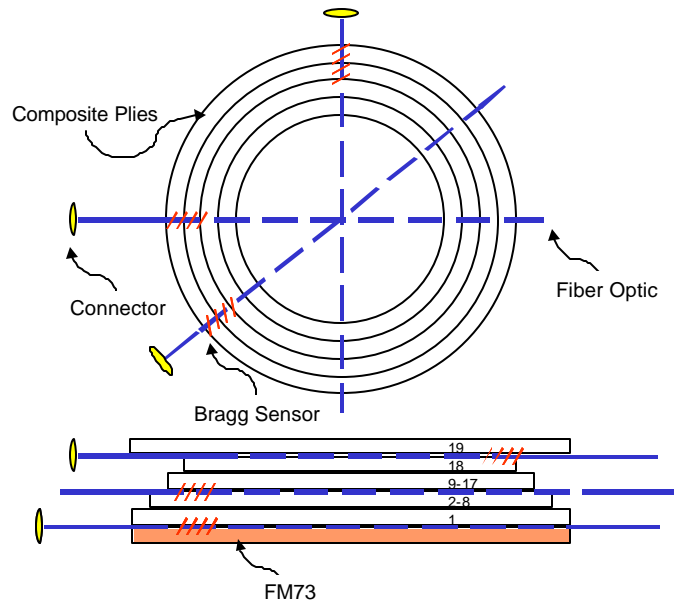


Figure 12. Scarfed Gr/Ep Patch Sensor Installation Schematic

All three sensors (0 deg, 45 deg and 90 deg) survived the installation and curing process. This included overlapping the fiber optics outside of the patch and under the thermal blankets. Data from the sensors were obtained during a series of loading conditions (figure 13) using an OSA with a resolution of 0.05nm. The loading conditions were:

- Load 1: no load;
- Load 2: man standing on top of the part (at ~105 Kg);
- Load 3: pallet jack loading on part while under stand (magnitude unknown);
- Load 4: pallet jack loading plus three men (~320 Kg extra); and
- Load 5: no load/residual (to verify return to initial condition).



Load 2



Load 3



Load 4

Figure 13. F-22 Panel Loading Conditions

Data from the three sensors in the patch all have the same general trend, however, there are differences in the output patterns due to slightly different loading conditions and directions. Plots of the results of the three sensors and the five loading conditions are contained in Figures 14, 15 and 16. All the sensors shifted to the left as the increasingly heavier loads were applied. There was also movement between the two peaks for each sensor, indicating a change in shear loading as well. The 0-degree sensor was broken through user error before the final two loads

could be applied, so no data could be recorded for loads 4 and 5. Note that the left axis is wavelength and the right axis is change in wavelength.

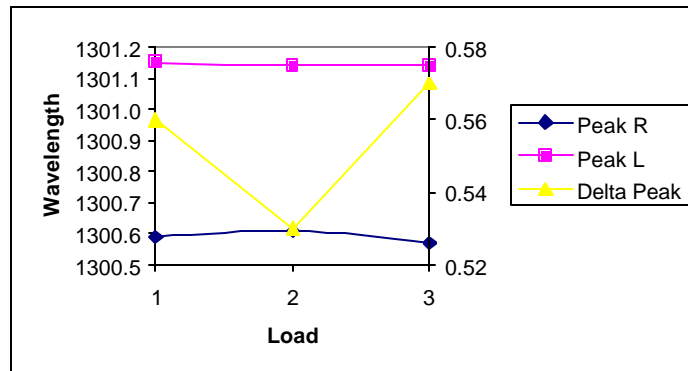


Figure 14. F-22 Panel, 0 Degree Sensor Data

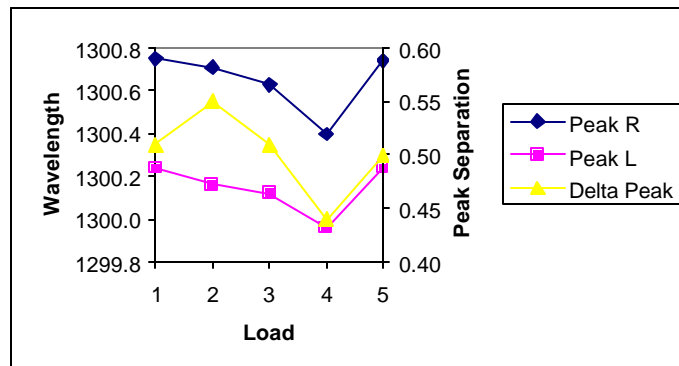


Figure 15. F-22 Panel, 90 Degree Sensor Data

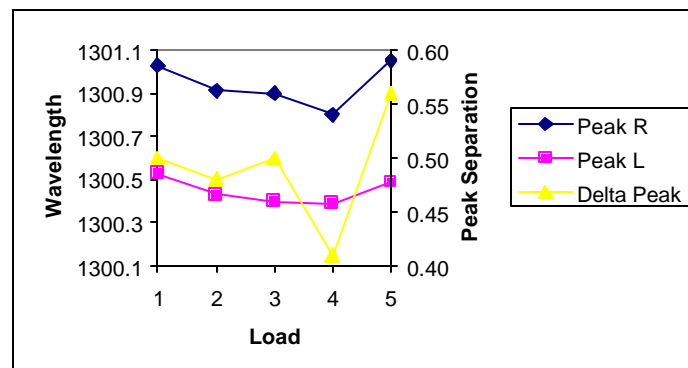


Figure 16. F-22 Panel, 45 Degree Sensor Data

Conclusions/Recommendations

This evaluation shows that it is possible to install fiber optic sensors in structural repair situations to record changes in strain (although not quantified in this effort) while the repair is being loaded. This includes both composite and metal bonded repair patches. The evaluation provided insight into the possible challenges that exist in installing the fibers in a repair and their vulnerability during the repair bonding process. It also provided insight into the type of data that

can be obtained (at least in its raw data format) and how that might possibly be correlated into strains for structural assessment of the repair.

When fibers are placed in either the bond line of a repair patch or the patch itself, several identifiers can be used to verify the repair's structural integrity. If the wavelength output shifts during loading, then strain is being detected, indicating that the load has been transferred to the patch. The shift in wavelength can be related to the amount of strain applied to the patch at the sensor location using the Bragg equation. If, during loading, the sensor indicates no shift in wavelength, then the patch is not carrying load due to a disbond or delamination and a non-destructive inspection should be performed. If the sensor fails this could also indicate a disbond, delamination or destruction of the bond, which requires investigation. If the sensor is a bi-axial sensor and aligned properly then shear or transverse loading may be measured as a change of wavelength separating the left and right peaks of the sensor output.

There are still many questions to be answered, however. This includes even fairly basic questions such as will the fiber optic sensors be able to provide the proper information during maintenance activities to assess repair integrity? The data obtained in this study showed that after failure, the sensor data returned to an unloaded condition. Thus, one would have to ensure that the sensor is sensitive enough to pick up differences in an unloaded (and failed) condition and one that contains residual strains imposed on the repair due to the thermal and surrounding structural loading when not in service (i.e. the airplane is on the ground). Another question is whether the sensor leads coming out of the repair should be external or should they be routed internally? External leads can be very vulnerable to damage due to maintenance and flight conditions, but may be able to be accessed easily and may be easier to install than internal leads. Internal leads, however, provide an opportunity for in-flight monitoring of the sensors. This data can be very useful for engineering assessment of the repair patch integrity. However, many structures may not lend themselves to installing the sensor leads internally.

Additional basic issues that need to be resolved are where and how many sensors should be installed, compatible connector types, sensor connection methods, recording/ data displaying equipment, and on who is the user of the data (technician or engineer). Due to the many questions that remain, further study of the utility of the fiber optic sensor for structural repairs needs to be performed.

References

- A. Vengsarkar, et. al., "Long-period fiber gratings as band-rejection filters," Journal of Lightwave Technology, 14, 58, (1996).
- K. O. Hill, et. al., "Photosensitivity in optical fiber waveguides: application to reflection filter fabrication," Appl. Phys. Lett., 32, (10), 647-649, (1978).
- W. Schulz, et. al., "Progress on Health Monitoring of An Adhesive Joint Using a Multi-Axis Fiber Grating Strain Sensor System," SPIE's International Symposium on NDE Techniques for Aging Infrastructure & Manufacturing Conference Proceedings, 3991-9, (2000).
- A. Trego, et. al., "Optical Fiber-Based Health Monitoring Systems for Composite Structures," AIAC, (2001).

Biographies

Angela Trego, Ph.D., P.E., is a Senior Specialist Engineer at Boeing Phantom Works in the Structures Technology group. Responsibilities include structural health monitoring, fiber optic sensor technology, corrosion assessment of aging aircraft structures and general dynamic analysis of structures. She is the author of 20 publications ranging from the development of passive damping techniques to the modeling of corrosion damage in structures. Dr. Trego graduated from Brigham Young University in 1997 with a Ph.D. in Mechanical Engineering and an emphasis in material science.

Russell Keller is a Senior Principal Engineer at Boeing in Seattle, WA. He is the lead engineer for structural repair development activities within the Advanced Support Concepts organization of Phantom Works. He has 14 years of experience in composite and battle damage repair development, including the disciplines involved with its design, analysis, materials, processes, and procedure development. He has authored eleven publications related to composite repairs. Mr. Keller graduated from the USAF Institute of Technology in 1986 with a Masters of Science in Aeronautical Engineering.